

Supplementary

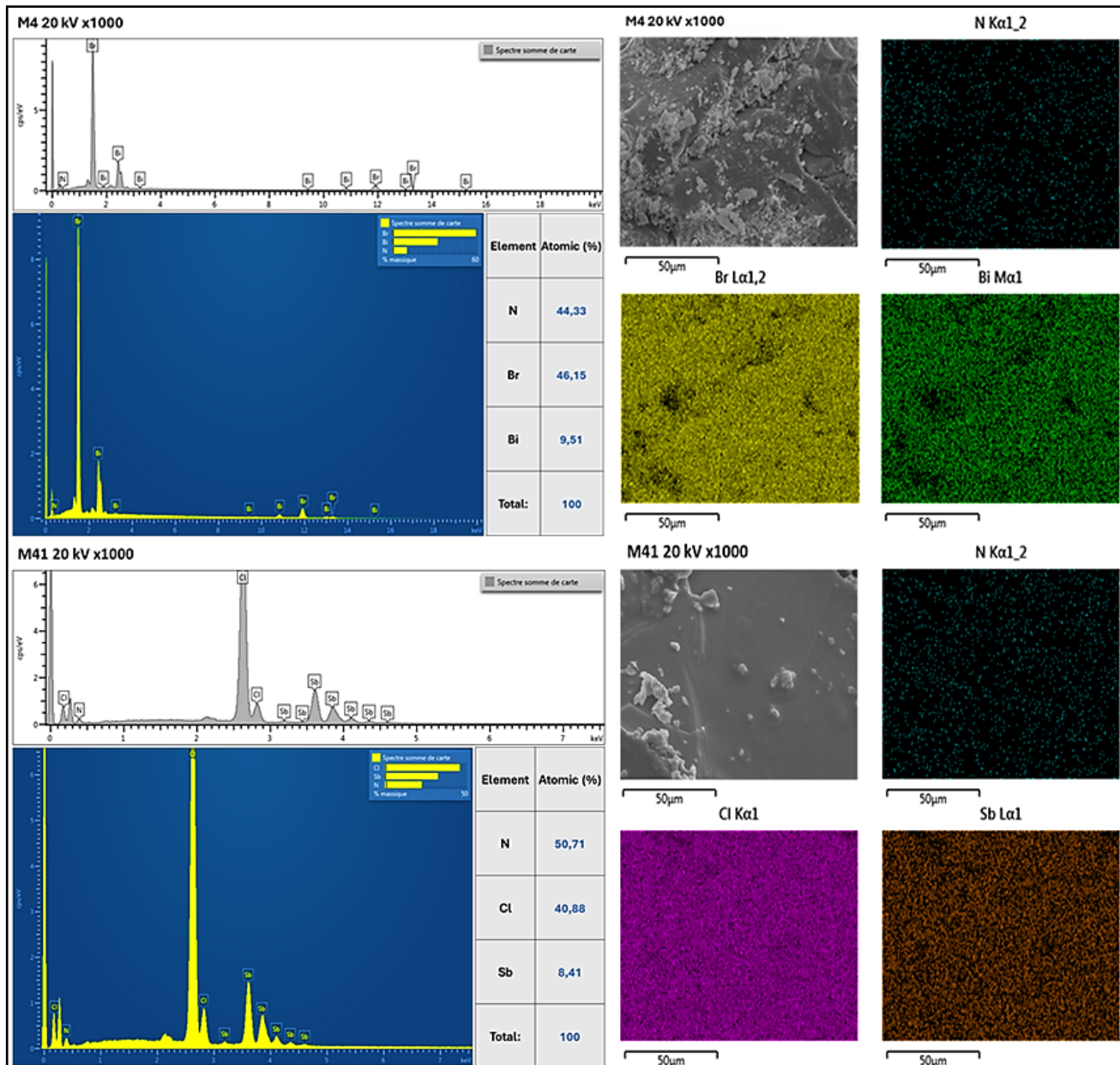


Fig. 1.S: EDS spectrum and elemental mapping of M4 and M41 compounds

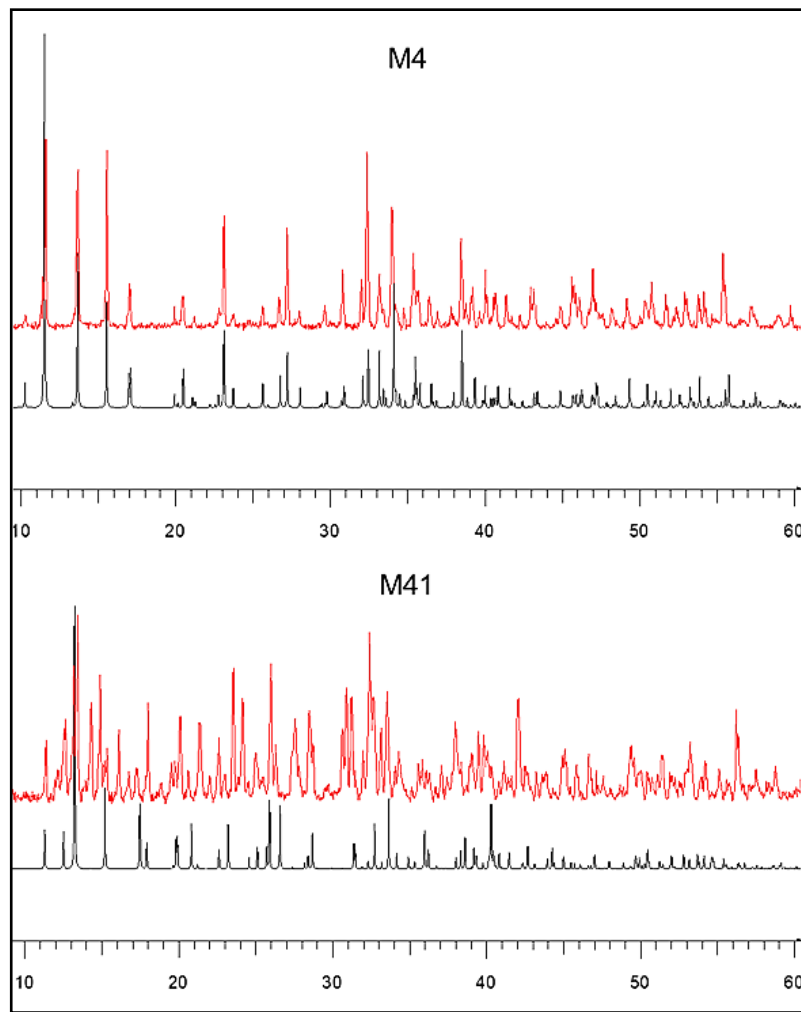


Fig. 2.S: PXRD pattern with experimental (red) and simulated (black) data of M4 and M41 compounds

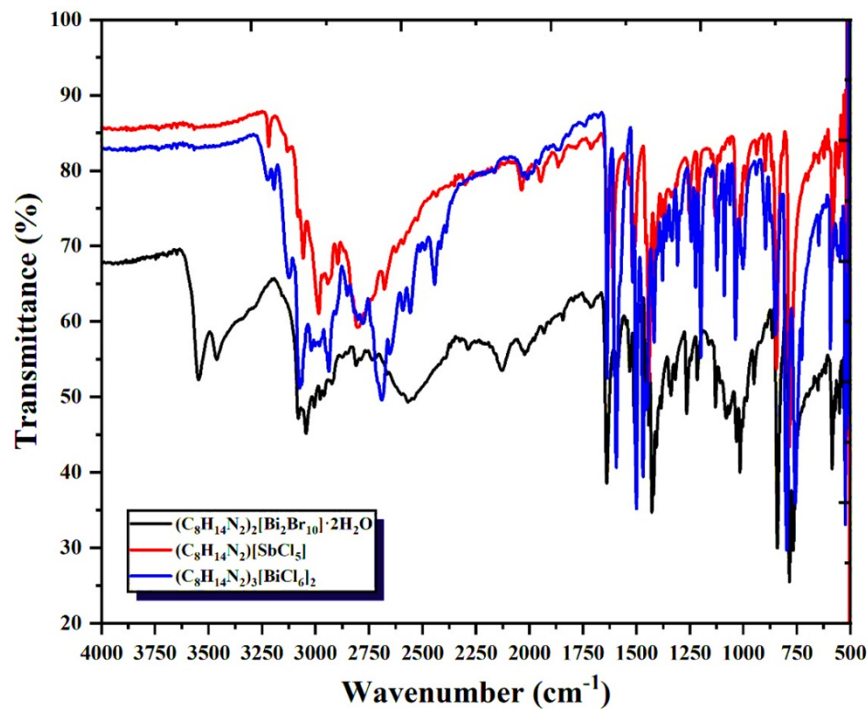


Fig. 3.S: Comparative FTIR Spectra of the three compounds

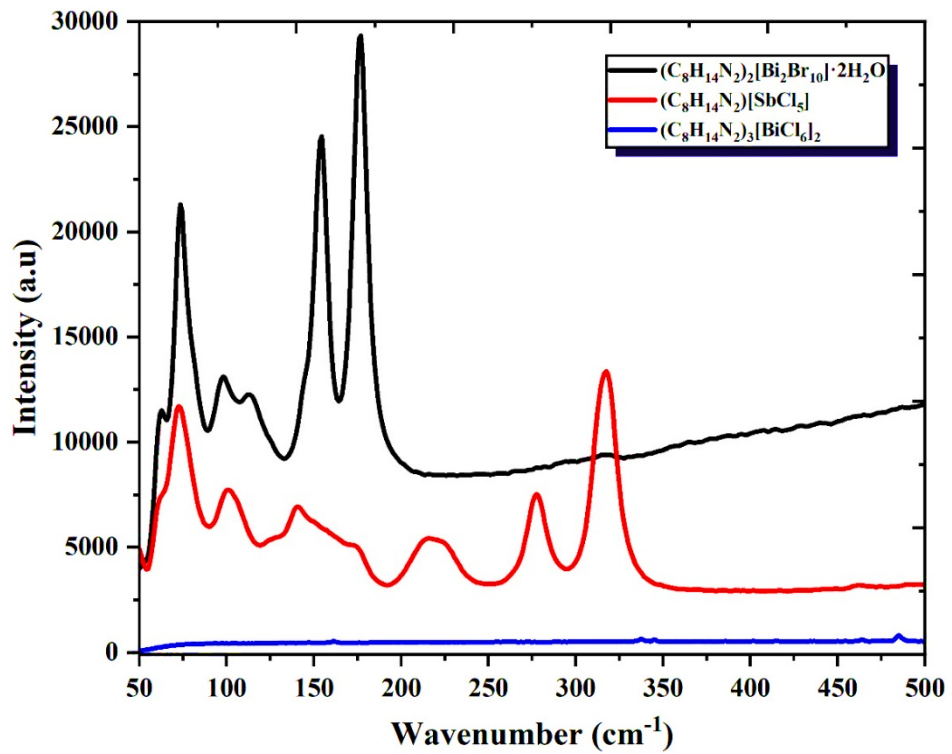


Fig. 4.S: Comparative Raman Spectra of the three compounds

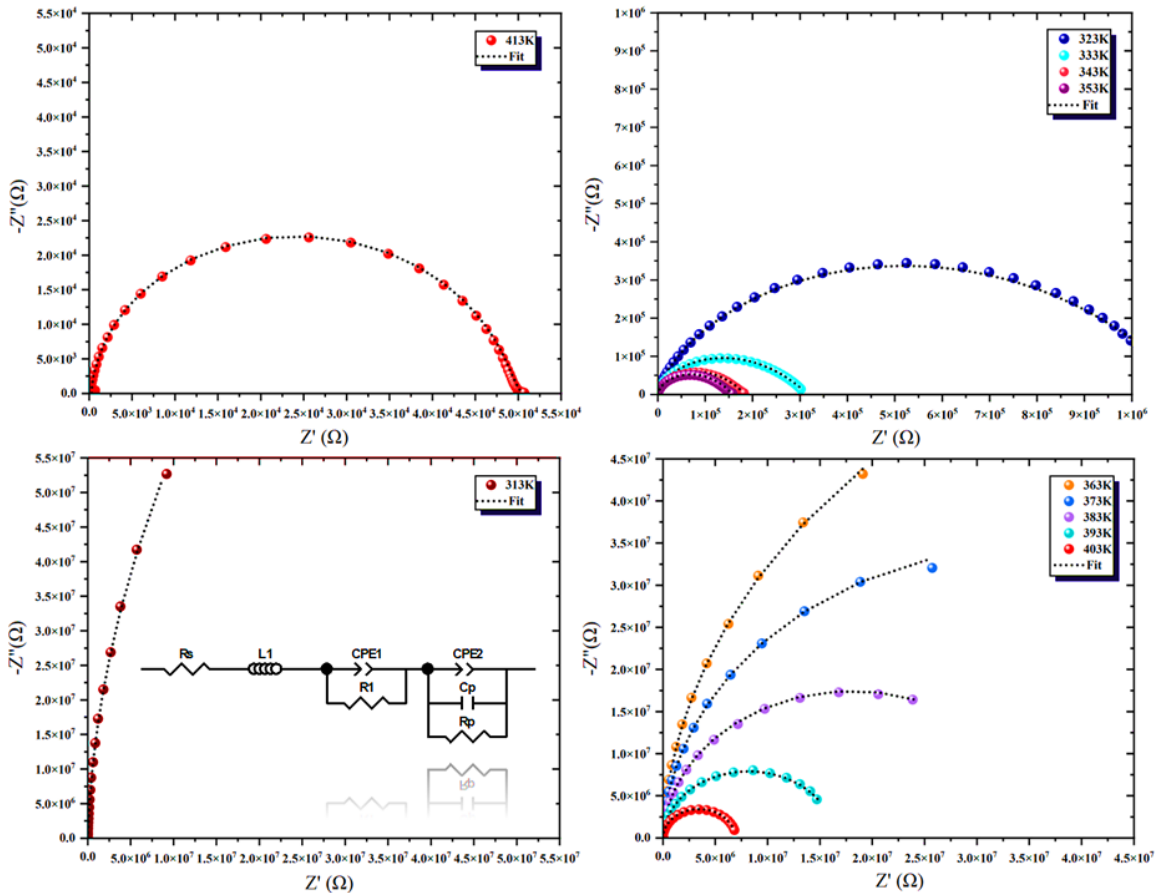


Fig. 5.S: Nyquist Plots at Different Temperatures ($-Z''$ vs Z')

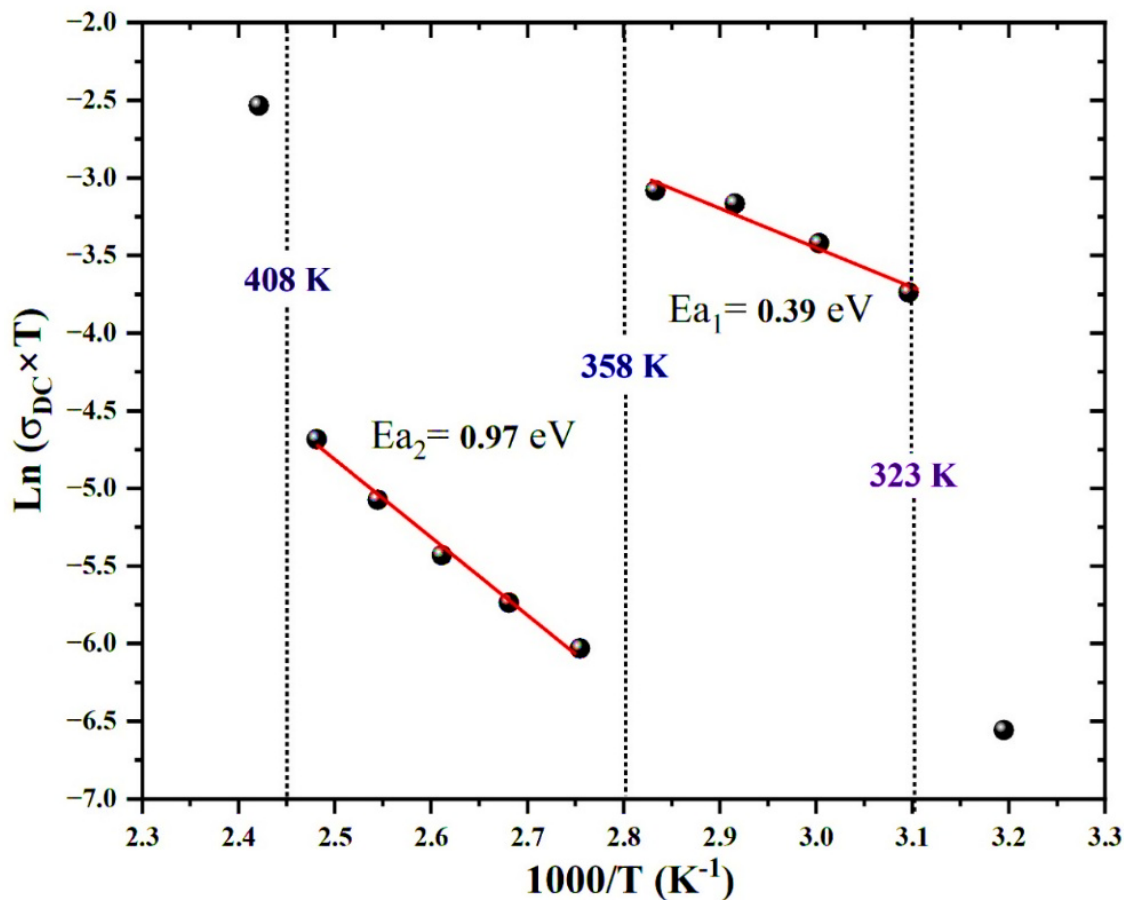


Fig. 6.S: Thermal Activation of Conductivity $\ln(\sigma \times T) = f(1000/T)$

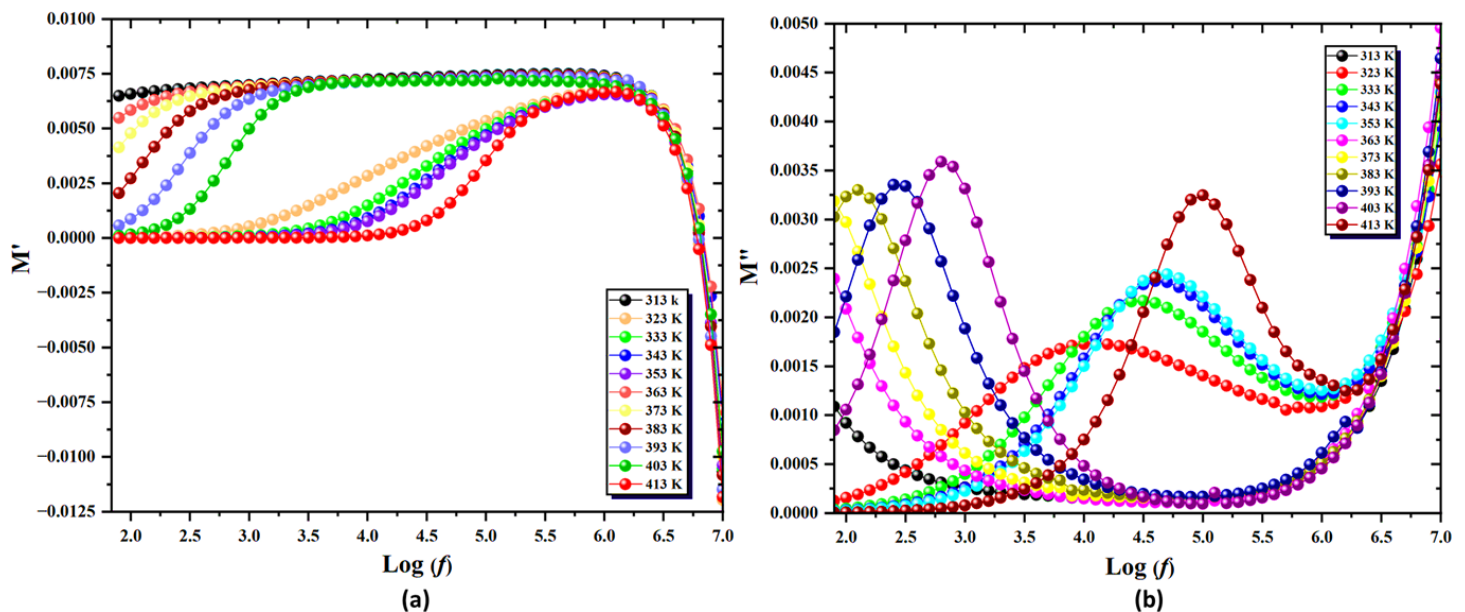


Fig. 7.S: Frequency Dependence of the Complex Electric Modulus: **(a)** Real Part (M') and **(b)** Imaginary Part (M'') as a Function of $\log(f)$ at Various Temperatures

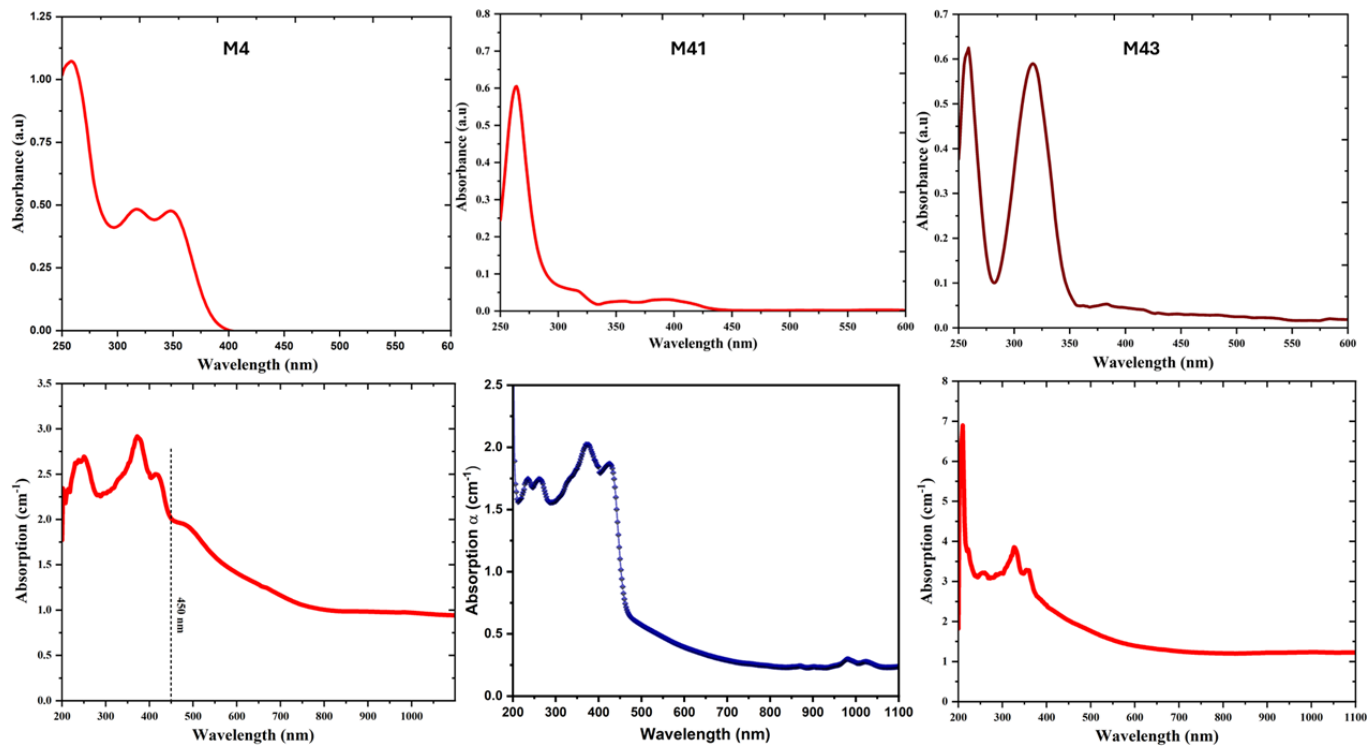


Fig. 8.S: Comparative aqueous- and solid-state UV–Vis spectra of the three compounds

Table 1.S: Crystallographic and structural features of the three hybrid halometalate compounds

Feature	$(C_8H_{14}N_2)_2[Bi_2Br_{10}] \cdot 2H_2O$	$(C_8H_{14}N_2)[SbCl_5]$	$(C_8H_{14}N_2)_3[BiCl_6]_2$
CCDC	2384365	2382366	2432091
Space Group	Monoclinic $P2_1/c$	Monoclinic $P2_1/n$	Triclinic $P\bar{1}$
Inorganic Unit	Dimeric $[Bi_2Br_{10}]^{4-}$	One Isolated $[SbCl_5]^{2-}$	Two Isolated $[BiCl_6]^{3-}$
Metal Coordination	Bi^{3+} : Octahedral with 6 Br^- (2 bridging)	Sb^{3+} : 5-coordinate, square-pyramidal	Bi^{3+} : Octahedral with 6 Cl^-
Bond Length Range	Bi–Br: 2.7271(5)–3.0612(5) Å	Sb–Cl: 2.4234(5)–2.9774(5) Å	Bi–Cl: 2.5965(16)–2.8387(17) Å
Distortion Cause	Very small distortion, in the order of 1.7×10^{-6}	geometry-inert $5s^2$ lone pair on Sb^{3+} with small distortion (4.53×10^{-3})	Somewhat between medium and small distortion (2.41×10^{-2} and 3.58×10^{-2}), due to $6s^2$ lone pair effect on Bi^{3+}
Dimensionality	0D (discrete dimers)	0D (pseudo-polymeric $SbCl_5$ chains)	0D (isolated octahedra)
Supramolecular Features	3D H-bonding with $N-H \cdots Br$ and $O-H \cdots Br$; water enhances cohesion	Semi-connected $N-H \cdots Cl$ H-bond network with pseudo-chains	Dense H-bonding via $N-H \cdots Cl$; solvent-free
Packing Description	Very Dense network; very compact, includes 2 lattice water molecules	Dense network, solvent-free, very compact, and efficient packing	Medium, solvent-free, somewhat compact, and efficient packing
Void Volume	5.9%	7.1%	10.2%
Influence of Metal & Halide	$Bi + Br \rightarrow$ the densest, very slightly distorted dimers, enhanced H-bonding	$Sb + Cl \rightarrow$ slightly distorted, low crystal void	$Bi + Cl \rightarrow$ somewhat slightly distorted octahedra, low symmetry, medium packing
Symmetry vs.	High symmetry, edge-sharing	High symmetry, distorted	Low symmetry, regular octahedra

Geometry	dimer	5-coordination	
H. Bonding Types	N–H···Br, O–H···Br	N–H···Cl	N–H···Cl

Table 2.S: Comparative antibacterial activity between halometalate hybrids and M41 and the cation

Compound	Method / Dose	<i>E. coli</i> (mm)	<i>P. aeruginosa</i> (mm)	Notes
$(C_6H_7NCl)_3[BiCl_6] \cdot H_2O$ (Ouerghi et al.) ²⁹	Disk diffusion, 100 μ g/disc	~12 (mm)	~9 (mm)	Moderate activity; halide identity and lattice compactness limit release.
$(H_2DDS)[Bi_4I_{16}]$ (Ben Ali et al.) ³⁰	Agar well, 1 mg/well	11 \pm 1.4 (mm)	8 (mm)	Iodide enhances polarizability, but framework rigidity restrains activity.
4-(ethylaminomethyl) pyridine	Agar well, 1 mg/well	31 (mm)	29 (mm)	Strong intrinsic antibacterial activity linked to aromatic cation release.
M41 ^{19,20}	Agar well, 1 mg/well	25–34 (mm)	25–34 (mm)	Synergistic lattice–cation contribution; markedly superior to comparable halobismuthates.
Gentamicin (control)	Agar well, 15 μ g/well	21–30 (mm)	21–30 (mm)	Clinically relevant benchmark; M41 shows competitive or superior efficacy.